cmgh
CELLULAR AND MOLECULAR GASTROENTEROLOGY AND HEPATOLOGY

RESEARCH LETTER

# Non-heat-stressed Method to Isolate Hepatic Stellate Cells From Highly Steatotic Tumor-bearing Liver Using CD49a

The number of patients with non-viral, nonalcoholic steatohepatitis-associated liver cancer has been increasing with the prevalence of obesity. Increasing evidence shows that the tumor microenvironment (TME) is crucial for tumor progression. We previously showed that hepatic stellate cells (HSCs) play key roles in tumorigenic TME of obesity-associated hepatocellular carcinoma (HCC) by secreting senescence-associated secretory factors that suppress anti-tumor immunity.[1-3] Recent advances in single-cell RNA-sequencing (scRNA-seq) techniques have enabled the characterization of different cell types in various tissues. Therefore, development of a refined method to characterize HSCs in TME under various conditions is necessary to understand their role in HCC progression.

Isolation of HSCs from normal liver via perfusion from the inferior vena cava (IVC) using a retrograde approach has been reported.[4] However, this method is not applicable to highly steatotic liver or steatohepatitic tumor tissues in obese mice as the accumulation of adipose tissue in obese mice hinders IVC visualization, thereby making cannulation via IVC difficult. Therefore, we attempted HSC isolation through the portal vein (PV), which is clearly visible under all conditions. We aimed to develop a method to isolate HSCs at a low temperature (6 °C) to minimize over digestion by enzymes and heat-associated stress after dissociation (at 37 °C), which reportedly induce genes such as *Fos* and *Jun*.[5] Furthermore, we identified a cell surface marker abundantly expressed in HSCs, which is useful for HSC cell sorting from murine and human liver tumor tissues.

In this proposed protocol, cannulation via PV and digestion using ice-cold enzymatic solution (Figure 1, *A*–*B*) are important steps for successful HSC isolation. We confirmed that the ice-cold enzyme solutions (pronase E, collagenase, and DNase I) retained enzymatic activity at 6 °C. The HSCs were concentrated using Nycodenz gradient medium (Supplementary Figure 1, *A*–*D*). The expression of *Lrat*, a marker for HSCs, revealed maximum HSC fraction in 13% Nycodenz gradient medium (Supplementary Figure 1, *A*). Pronase E was used to destruct hepatocytes,[6] and almost no live hepatocyte contamination was confirmed. In contrast, increased contamination with macrophages (*Clec4f* expressing cells) and liver sinusoidal endothelial cells (LSECs, *Stab2* expressing cells) was observed at higher concentrations of Nycodenz (Supplementary Figure 1, *B*–*C*). Therefore, we decided to use 13% Nycodenz gradient medium for the subsequent experiments including flow cytometry and cell sorting.

To screen HSC-specific cell surface markers, we sorted $CD31^-/CD45^-$ cells from the HSC-rich 13% Nycodenz fraction and performed scRNA-seq using the $CD31^-/CD45^-$ fraction, excluding LSECs and immune cells (Figure 1, *C*). In the t-distributed stochastic neighbor embedding (t-SNE) analysis (Figure 1, *D*), clusters 0, 1, 2, and 6 predominantly expressed *Lrat*, indicating that they were HSC fractions (Figure 1, *E*). However, the other clusters consisted mainly of hepatocytes and HCC cells (*Hnf4a*-expressing cells), but almost no cholangiocytes (*Krt19*-expressing cells) were observed (Supplementary Figure 2, *A*). Among the top 50 genes expressed in the HSC clusters, we focused on 11 genes encoding cell surface molecules expressed in HSCs obtained from the livers of normal diet (ND)-fed mice (clusters 0 and 6 in Figure 1, *E*) and in those obtained from non-tumor (NT) (cluster 1) and tumor (T) (cluster 2) segments of high-fat diet (HFD)-fed mice (Supplementary Figure 2, *B*). All 3 segments comprised *Itga1* (encoding integrin alpha1, CD49a in CD classification), indicating that *Itga1* was the most commonly expressed surface molecule gene. Moreover, *Itga1* distribution highly overlapped with *Lrat* distribution in the HSC clusters (Figure 1, *F*), indicating that *Itga1* (CD49a) could be an excellent HSC cell surface marker in the livers of both ND-fed and HFD-induced HCC-bearing mice. Therefore, we sorted the CD49a-high cell population among $CD31^-/CD45^-$ cells (Supplementary Figure 1, *E*; Figure 1, *G*) and conducted scRNA-seq analysis. *Itga1* (CD49a) was confirmed as a promising HSC marker comparable to *Lrat* (Figure 1H), and there was almost no contamination of other liver cell types. Furthermore, the content of retinoid, a reported HSC marker in normal liver,[4] was significantly reduced by HFD-induced tumor progression, whereas high CD49a expression was maintained (Supplementary Figure 2, *C*), indicating that CD49a could be used as an HSC marker under various conditions.

The heat-stress response and related modulation in gene expression occur following enzymatic digestion at 37 °C.[5,7] To evaluate the side effects of high-temperature enzyme incubation on transcriptome, bulk RNA-sequencing of 24346 genes of CD49a-high HSCs was performed at 37 °C or 6 °C, and the results were compared. A total of 3071 genes were overexpressed at 37 °C compared with those at 6 °C (Figure 1, *I*). Subsequently, pathway enrichment analysis was performed on 1144 commonly overexpressed genes. Notably, expression of several ribosomal genes, which reflects stress-mediated translation,[8] was upregulated (Figure 1, *J*). We identified the top 20 co-expressed genes. The common stress responsive transcription factor *Atf3* and prototypical immediate-early response genes (*Fos* and *Jun* gene families) were overexpressed at 37 °C (Figure 1, *K*).

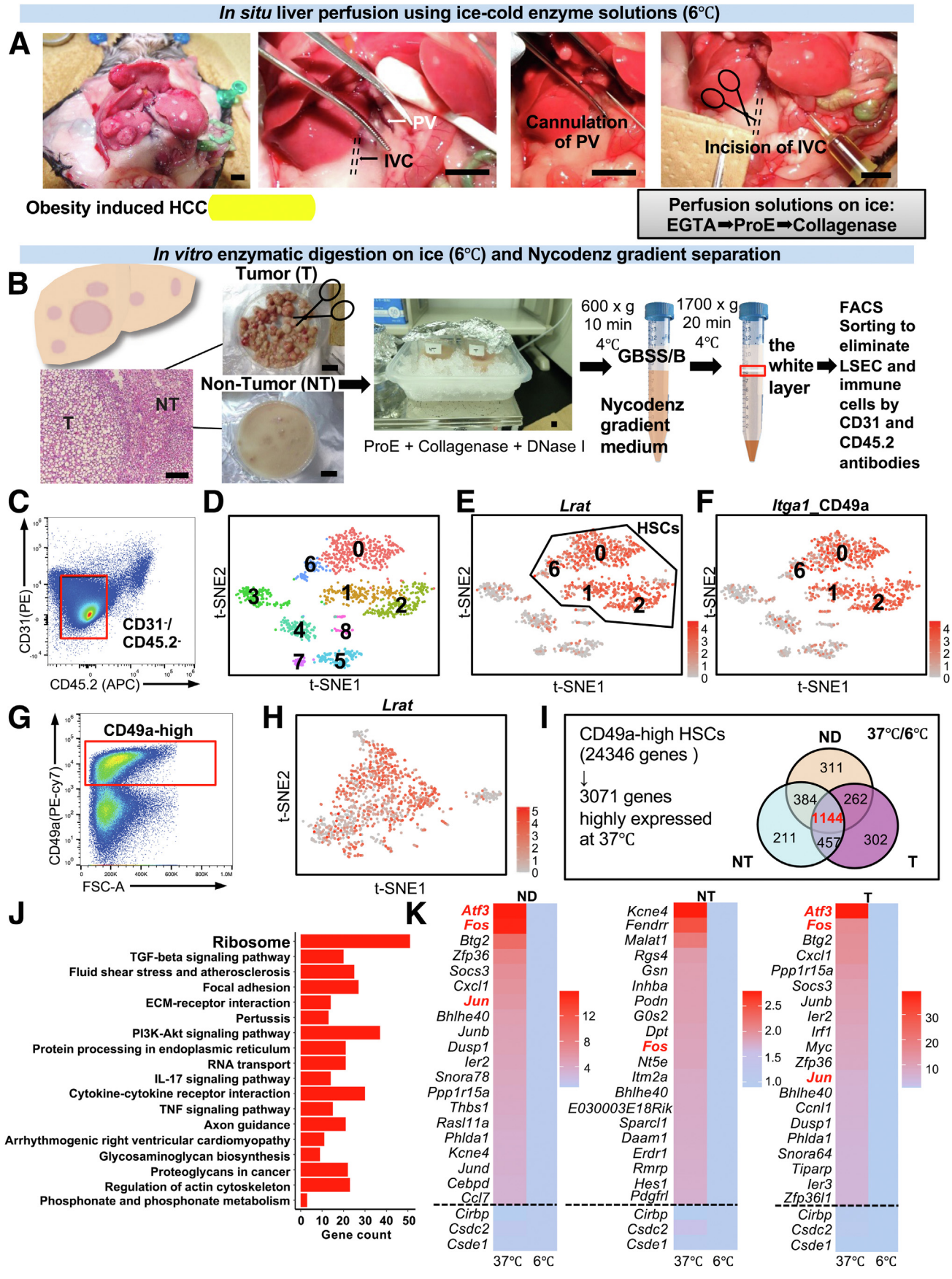
In situ liver perfusion using ice-cold enzyme solutions (6℃)
A
PV
IVC
Cannulation of PV
Incision of IVC
Obesity induced HCC
Perfusion solutions on ice:
EGTA➡ProE➡Collagenase
In vitro enzymatic digestion on ice (6℃) and Nycodenz gradient separation
B
Tumor (T)
Non-Tumor (NT)
T
NT
ProE + Collagenase + DNase I
600 x g
10 min
4℃
GBSS/B
Nycodenz gradient medium
1700 x g
20 min
4℃
the white layer
FACS Sorting to eliminate LSEC and immune cells by CD31 and CD45.2 antibodies
C
CD31(PE)
CD45.2 (APC)
CD31-/ CD45.2-
D
t-SNE2
t-SNE1
E
Lrat
HSCs
F
Itga1_CD49a
G
CD49a-high
CD49a(PE-cy7)
FSC-A
H
Lrat
I
CD49a-high HSCs (24346 genes )
3071 genes highly expressed at 37℃
ND
37℃/6℃
311
384
262
1144
211
457
302
NT
T
J
Ribosome
TGF-beta signaling pathway
Fluid shear stress and atherosclerosis
Focal adhesion
ECM-receptor interaction
Pertussis
PI3K-Akt signaling pathway
Protein processing in endoplasmic reticulum
RNA transport
IL-17 signaling pathway
Cytokine-cytokine receptor interaction
TNF signaling pathway
Axon guidance
Arrhythmogenic right ventricular cardiomyopathy
Glycosaminoglycan biosynthesis
Proteoglycans in cancer
Regulation of actin cytoskeleton
Phosphonate and phosphonate metabolism
Gene count
K
ND
Atf3
Fos
Btg2
Zfp36
Socs3
Cxcl1
Jun
Bhlhe40
Junb
Dusp1
Ier2
Snora78
Ppp1r15a
Thbs1
Rasl11a
Phlda1
Kcne4
Jund
Cebpd
Ccl7
Cirbp
Csdc2
Csde1
37℃ 6℃
NT
Kcne4
Fendrr
Malat1
Rgs4
Gsn
Inhba
Podn
G0s2
Dpt
Fos
Nt5e
Itm2a
Bhlhe40
E030003E18Rik
Sparcl1
Daam1
Erdr1
Rmrp
Hes1
Pdgfrl
Cirbp
Csdc2
Csde1
37℃ 6℃
T
Atf3
Fos
Btg2
Cxcl1
Ppp1r15a
Socs3
Junb
Ier2
Irf1
Myc
Zfp36
Jun
Bhlhe40
Ccnl1
Dusp1
Phlda1
Snora64
Tiparp
Ier3
Zfp36l1
Cirbp
Csdc2
Csde1
37℃ 6℃

Furthermore, the enrichment analysis revealed upregulation of other stress response pathways such as ER stress signaling and inflammatory pathways under heat-stressed conditions. Nevertheless, the expression of cold shock protein-encoding genes including *Cirbp, Csds1*, and *Csds2* remained unchanged (Figure 1, *K*), suggesting that HSC isolation at 6 °C could minimize the generation of enzyme and heat-stressed transcriptional artefacts.

We applied this protocol to collect HSCs with high CD49a expression from the livers of *db/db* mice (a well-established obese model) (Supplementary Figure 3, *A*) and confirmed the high yield and high purity of HSCs based on *Lrat* expression. We also applied this protocol to isolate HSCs from human HCC tissue (T-hHSCs) (Supplementary Figure 3, *B–C*). Consistent with murine HSCs, human HSCs from HCC tissue were confirmed as a CD49a-high population among $CD31^-$/ $CD45^-$ cells. The mRNA expression of *ACTA2* suggested that T-hHSCs predominantly consisted of activated HSCs as we observed previously[1,2] (Supplementary Figure 3, *D*).

In conclusion, we developed a method to isolate HSCs from highly steatotic liver and steatohepatic HCC tissues utilizing PV-mediated enzymatic cold perfusion method to avoid heat-induced artefact gene expression. Furthermore, we identified CD49a as a reliable HSC marker under various conditions in this procedure. These results lay a foundation for investigating the role of HSCs in liver under both normal and steatotic HCC conditions.

*YI CHENG*[*]
*RYOTA YAMAGISHI*[*]
*YOSHIKI NONAKA*
Department of Pathophysiology
Graduate School of Medicine
Osaka Metropolitan University
(formerly Osaka City University)
Osaka, Japan

*MISAKO SATO-MATSUBARA*
*NORIFUMI KAWADA*
Department of Hepatology
Graduate School of Medicine
Osaka Metropolitan University
(formerly Osaka City University)
Osaka, Japan

*NAOKO OHTANI*
Department of Pathophysiology, Graduate School of Medicine, Osaka Metropolitan University (formerly Osaka City University), Osaka, Japan *and*
AMED-CREST, Japan Agency for Medical Research and Development (AMED), Tokyo, Japan

## References

1. Yoshimoto S, et al. Nature 2013;499:97–101.
2. Loo TM, et al. Cancer Discov 2017;7:522–538.
3. Schwabe RF, et al. J Hepatol 2020;72:230–238.
4. Mederacke I, et al. Nat Protoc 2015;10:305–315.
5. O'Flanagan CH, et al. Genome Biol 2019;20:210.
6. Werner M, et al. PLoS One 2015;10:e0138655.
7. Adam M, et al. Development 2017;144:3625–3632.
8. Vind AC, et al. Nucleic Acids Res 2020;48:10648–10661.

[*]**Authors share co-first authorship.**

***Abbreviations used in this paper:*** **HCC, hepatocellular carcinoma; HFD, high-fat diet; HSC, hepatic stellate cell; IVC, inferior vena cava; LSECs, liver sinusoidal endothelial cells; ND, normal diet; NT, non-tumor; PV, portal vein; scRNA-seq, single-cell RNA-sequencing; T, tumor; T-hHSCs, HSCs from human HCC tissue; TME, tumor microenvironment; t-SNE, t-distributed stochastic neighbor embedding.**

**Most current article**



**2352-345X**
**https://doi.org/10.1016/j.jcmgh.2022.07.006**

**Received December 29, 2021. Accepted July 11, 2022.**

**Correspondence**
Address correspondence to: Naoko Ohtani, MD, PhD, Department of Pathophysiology, Graduate School of Medicine, Osaka Metropolitan University, Osaka, Japan. e-mail: naoko.ohtani@omu.ac.jp.

**Acknowledgments**
The authors thank Dr. Yoshimi Yukawa-Muto and the Department of Surgery for their help in collecting human samples used in this study. We thank Dr. Tomonori Kamiya and the laboratory members of Pathophysiology for their technical assistance. This manuscript has been edited by English editing company, Editage, which was supported by the Takeda Science Foundation.

**Conflicts of interest**
The authors disclose no conflicts.

**Funding**
This study was funded by AMED (Japan Agency for Medical Research and Development), under grant numbers JP20gm1010009 (Naoko Ohtani and Norifumi Kawada), JP20fk0210050 (Norifumi Kawada) and JP19ck0106260 (Naoko Ohtani). This study was also supported by the Japan Society for the Promotion of Science (JSPS) under grant numbers 19H04002 (Naoko Ohtani), 19H03641 (Norifumi Kawada), 21K07968 (Misako Sato-Matsubara), and 20K16309 (Ryota Yamagishi) as well as a grant from Takeda Science Foundation (Naoko Ohtani) and Yakult Bio-Science Foundation (Naoko Ohtani), and Research Grant of the Princess Takamatsu Cancer Research Fund 18-25003 (Naoko Ohtani).

**Figure 1.** (***See previous page***). **Cold perfusion method for isolating HSCs minimising heat-induced artefact gene expression.** CD49a is a useful HSC marker. *A*, The cannulation of liver via portal vein and incision of the inferior vena cava were performed in obesity-induced HCC mice (scale bars, 6 mm). The liver was perfused sequentially with EGTA, Pronase E (ProE), and collagenase. *B*, The histology of steatotic liver tumor in mice (hematoxylin and eosin staining, scale bar, 200 $\mu$m). In vitro enzymatic digestion and Nycodenz gradient separation. *C*, Flow cytometry plots for sorting $CD31^-/CD45.2^-$ cells from livers of ND- and HFD-induced HCC mice. n = 6, 35 w, (3 ND mice; 3 HCC mice). The average mouse body weight (BW): ND, 36.3 g (range, 35–38 g); HCC, 58.4 g (range, 55–61 g). *D*, t-SNE plots of cell clusters based on single-cell transcriptomes. *E*, Unsupervised clustering analysis identified HSC clusters based on *Lrat* expression. *F*, Unsupervised clustering analysis of *Itga1* among $CD31^-/CD45.2^-$ cells. *G*, Flow cytometry plots for sorting CD49a-high cells among $CD31^-/CD45.2^-$ cells from livers of HFD-induced HCC mice. n = 6, 35 w, (3 ND mice; 3 HCC mice). The average mouse body weight (BW): ND, 31.5 g (range, 30–33 g); HFD, 53.2 g (range, 45–57 g). *H*, Consistent unsupervised clustering analysis of *Lrat* using CD49a-high cells among $CD31^-/CD45.2^-$ cells. *I*, Bulk RNA-sequencing analysis of CD49a-high HSCs of ND, NT, and T tissues. n = 12, 35 w, (6 ND mice; 6 HCC mice). The average mouse body weight (BW): ND, 31.7 g (range, 28–34 g); HCC, 57.6 g (range, 51–64 g). *J*, Pathway enrichment analysis of the 1144 common highly expressed genes using Enrichr. *K*, Heatmap of the top 20 commonly overexpressed genes (above the dotted line) at 37 °C among the ND, NT, and T datasets. Heat map of the cold shock genes (below the dotted line) among the ND, NT, and T datasets.

# Supplementary Methods

## Mice and Diet

C57BL/6 mice (CLEA Japan) and the 2 diets (normal diet, CE2; CLEA Japan and a high-fat diet [HFD], D12492; Research Diet) were used.[1] Obese mice (>45 g; 30–40 weeks) were used in accordance with the protocols approved by the Animal Care and Use Committee of Osaka City University (Approval number: 17206). Chemically induced liver carcinogenesis was performed as described previously.[1]

## Isolation of Primary Hepatic Stellate Cells (HSCs)

The mice were anesthetized, and the portal vein was cannulated. After confirming the blood backflow, the catheter was connected to the perfusion line with EGTA perfusion solution (all solutions shown in Supplementary Table 1 should be ice-cold). As circulation started, the inferior vena cava was cut to discard the perfused solution. The perfusion was sequentially performed using 35, 60, and 75 mL of EGTA, Pronase E (Sigma), and collagenase (Wako) solutions until the entire liver swelled up and softened (Figure 1, *A*). The liver was then explanted into a 10-cm dish on ice and soaked with enzyme buffer. Next, the non-tumor (NT) and tumor (T) sections were separated carefully. The NT sections turned fluid-like with pipetting, whereas the T sections remained solid and had to be minced (Figure 1, *B*). They were then transferred into 2 beakers with 45 mL of in vitro digestion solution and incubated for 30 minutes (6° C). The incubated tissues were filtered through a 70-$\mu$m cell-strainer into two 50-mL tubes (NT and T), centrifuged at 600 $\times$ *g* for 10 minutes (4 °C), and the pellet was re-suspended in GBSS/B. Nycodenz (AXS) solution (0.286 g/mL) was prepared by vortexing before use. The Nycodenz gradient medium (6%–17%) was prepared, and 8 mL of cell-Nycodenz gradient medium (with the ratio shown in Supplementary Figure 1, *D*) was transferred into moistened 15-mL tubes and overlaid with 3 mL of GBSS/B. The solutions were then centrifuged at 1700 $\times$ *g* for 20 minutes (accel & brake 0; 4 °C). A white intermedia layer of cells containing HSCs was obtained. A fat layer on the top was aspirated to avoid contamination. The white layer was collected and added into 40 mL of GBSS/B and subjected to low-speed centrifugation (50 $\times$ *g* for 5 minutes) to exclude hepatocytes. The supernatant was centrifuged at 1000 $\times$ *g* for 10 minutes (4 °C); thereafter, 3 mL of RBC lysis buffer (1×, Biolegend) was added to the pellet and incubated for 4 minutes to remove the erythrocytes, and then 2% fetal bovine serum (FBS)-phosphate buffered saline (PBS) was added to make up the volume to 14 mL for ceasing the reaction. Another step of high-speed centrifugation was performed at 1000 $\times$ *g* for 10 minutes (4 °C), and the pellet containing primary HSCs was re-suspended in 2% FBS-PBS solution and used for quantitative polymerase chain reaction (PCR), flowcytometry, and RNA-sequencing (RNA-seq). Although the yield of HSCs slightly varied in different mice, we could always isolate more than $10^6$ cells from one ND mouse liver regardless of mouse age (Supplementary Figure 1, *F*) and 10 $\times$ $10^6$ cells from the NT region and $10^6$ cells from the T region of one HFD-fed mouse liver.

## Quantitative PCR

Total RNA was extracted from primary HSCs using RNAiso Plus (Takara) and reverse-transcription and quantitative PCR were performed as previously described.[1] The primer sequences are listed in Supplementary Table 1.

## Flowcytometry and Sorting of HSCs

The isolated HSCs were pre-incubated with unlabelled anti-CD16/32 mAb (BioXcell) to avoid non-specific binding to FcγR. The cells were stained with antibodies against CD31, CD45.2, and CD49a (Biolegend), and analyzed using the Attune NxT Cytometer (Thermo-Fisher Scientific); and sorted using the SONY-SH800 cell sorter (SONY). Data were processed using FlowJo-Version-10 software. Dead cells were excluded using propidium iodide (Biolegend) gating. Antibodies used are listed in Supplementary Table 1.

## Single-cell RNA-seq

$CD31^-/CD45.2^-$ cells from ND, NT, and T of mouse livers were sorted for single-cell RNA-seq. Single-cell dispensing and library preparation were performed according to the protocol of the ICELL8 cx 3′ DE kit.[2] Libraries were sequenced on Illumina Novaseq 6000 with 25–150-bp paired-end reads to produce an average read of 934,102/cell. RNA-seq data of 1613 cells were obtained. The expression level of target genes in each cell was calculated using the mappa analysis pipeline (Demuxer and analyser version 1.0, ICELL8). From the gene expression matrix, quality control, data clustering, visualization, and differential expression analysis were performed using Seurat version 2.3.4 in R.[3] The HSC clusters were confirmed using t-SNE of marker gene expression, including *DES* (desmin), *CYGB* (cytoglobin), and *Lrat*. CD49a-high cells among $CD31^-/CD45.2^-$ cells from ND, NT, and T tissues of mouse livers were sorted for single-cell RNA-seq (ICELL 8, Takara). The libraries were sequenced to produce an average read of 892086/cell and RNA-seq data of 1390 cells were obtained. The expression level of target genes in each cell was calculated using the Cogent NGS Analysis Pipeline.

## Bulk RNA-seq

The total RNA was extracted from sorted-CD49a-high cells among $CD31^-/CD45.2^-$ cells using TRIzol (Invitrogen). Bulk RNA-seq libraries were prepared using the SMART-Seq v4 protocol (Takara). The libraries were sequenced on Illumina Hiseq4000. For each sample, depths of at least 27.6 million paired-end reads were generated. Mapping was performed using tophat. The expression level was calculated using cuffdiff and feature counts. From the gene

expression matrix, differential expression analysis was performed with R version 3.6.3.

### Human Subjects

The liver tumor tissue (approximately 5 × 5 × 5 $mm^3$ tissue), obtained from a patient with HCC who underwent partial hepatectomy, was minced and stirred with enzymes for 40 minutes (6 °C), and separated following the same procedure as the murine cell isolation method. We used 20% Nycodenz gradient medium to harvest the maximum number of cells from the limited tumor tissues. Thereafter, CD49a-high cells among $CD31^-$/$CD45.2^-$ cells were isolated. We isolated 7.3 × $10^5$ HSCs labelled as T-hHSCs. The study was conducted following the Helsinki Declaration II; written informed consent was obtained from each patient according to the protocol approved by the ethics committee of Osaka City University (Approved number: 3722).

### Data and Code Availability

The RNA-seq data are available in the GEO databases (accession numbers: HSCs at 37°C or 6°C: GSE192598, $CD31^-$/$CD45.2^-$/$CD49a^+$ HSCs: GSE192582, and CD31-/CD45.2-HSCs: GSE192637)

## References

1. Yoshimoto S, et al. Nature 2013;499:97–101.
2. Takara Bio. ICELL8 cx 3′ DE Kit User Manual. 32.
3. Butler A, et al. Nat Biotechnol 2018;36:411–420.

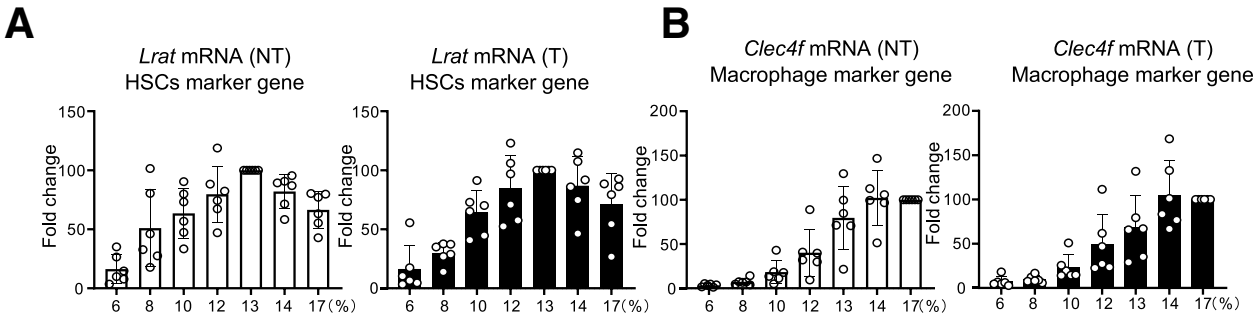


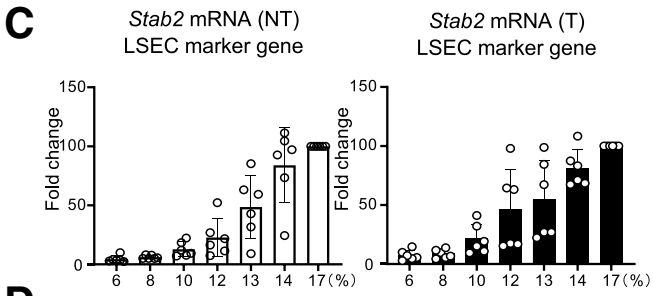


| Lrat/GAPDH | Nycodenz | 6% | 8% | 10% | 12% | 13% | 14% | 17% |
|---|---|---|---|---|---|---|---|---|
| NT | #1 | 7.7944 | 27.5112 | 47.3347 | 67.2357 | 100 | 86.9493 | 80.3167 |
| | #2 | 26.5583 | 101.469 | 90.3501 | 82.3197 | 100 | 89.2941 | 79.8104 |
| | #3 | 9.84728 | 32.814 | 73.2383 | 88.2043 | 100 | 90.629 | 77.0734 |
| | #4 | 3.53586 | 17.7498 | 33.4454 | 47.0376 | 100 | 58.3121 | 55.2919 |
| | #5 | 35.1339 | 80.4467 | 79.8536 | 118.81 | 100 | 71.4175 | 42.829 |
| | #6 | 14.7123 | 46.1269 | 56.8011 | 74.3853 | 100 | 95.3842 | 63.1176 |
| | mean | 16.2637 | 51.0195 | 63.5039 | 79.6654 | 100 | 81.9977 | 66.4065 |
| T | #1 | 10.374 | 28.8988 | 65.2018 | 122.981 | 100 | 85.8841 | 88.4186 |
| | #2 | 17.4179 | 34.9412 | 70.1052 | 70.9037 | 100 | 107.44 | 86.0919 |
| | #3 | 3.3791 | 37.6 | 44.6156 | 52.4716 | 100 | 114.759 | 79.3364 |
| | #4 | 4.60495 | 13.8746 | 40.7611 | 57.4921 | 100 | 46.2842 | 26.7422 |
| | #5 | 55.5332 | 37.2853 | 91.2588 | 105.906 | 100 | 74.779 | 54.3357 |
| | #6 | 6.53252 | 26.985 | 72.8805 | 96.9218 | 100 | 91.8666 | 92.7234 |
| | mean | 16.307 | 29.9308 | 64.1372 | 84.446 | 100 | 86.8354 | 71.2747 |
| Clec4f/GAPDH | NT | | | | | | | |
| | #1 | 1.60407 | 4.73271 | 11.262 | 31.9634 | 71.1756 | 99.345 | 100 |
| | #2 | 5.27147 | 6.66139 | 5.05625 | 9.44253 | 21.4703 | 51.3516 | 100 |
| | #3 | 1.20675 | 3.8306 | 18.7582 | 39.6928 | 70.595 | 96.664 | 100 |
| | #4 | 3.10704 | 7.11811 | 13.5289 | 29.8535 | 99.5881 | 105.736 | 100 |
| | #5 | 4.72676 | 14.1464 | 43.0323 | 88.8705 | 129.466 | 146.752 | 100 |
| | #6 | 3.90046 | 7.40401 | 17.8256 | 40.8416 | 84.599 | 112.54 | 100 |
| | mean | 3.30276 | 7.31553 | 18.2439 | 40.1107 | 79.4822 | 102.065 | 100 |
| T | #1 | 6.6968 | 12.227 | 19.4385 | 61.7416 | 79.3777 | 101.175 | 100 |
| | #2 | 4.5867 | 7.49858 | 14.1031 | 27.1101 | 66.9966 | 132.686 | 100 |
| | #3 | 4.60245 | 5.69413 | 14.5377 | 23.5543 | 35.2266 | 66.7578 | 100 |
| | #4 | 6.13365 | 8.87888 | 14.7733 | 22.5003 | 28.9417 | 76.6885 | 100 |
| | #5 | 18.116 | 16.7141 | 50.8896 | 111.503 | 131.781 | 168.466 | 100 |
| | #6 | 2.81374 | 8.10603 | 25.5778 | 46.8312 | 65.6887 | 83.3284 | 100 |
| | mean | 7.15823 | 9.85312 | 23.22 | 48.8734 | 68.0021 | 104.85 | 100 |
| Stab2/GAPDH | NT | | | | | | | |
| | #1 | 3.44071 | 4.97695 | 6.99122 | 11.3985 | 42.778 | 111.265 | 100 |
| | #2 | 9.90235 | 7.77005 | 7.71775 | 7.40495 | 9.03255 | 24.3987 | 100 |
| | #3 | 2.4219 | 5.02614 | 12.0541 | 21.7908 | 31.7024 | 73.4438 | 100 |
| | #4 | 3.55517 | 5.50562 | 9.40311 | 16.3404 | 63.1266 | 104.53 | 100 |
| | #5 | 4.03833 | 8.07975 | 22.2827 | 52.2274 | 85.2317 | 92.6338 | 100 |
| | #6 | 2.85766 | 5.03958 | 18.3645 | 26.828 | 59.2947 | 97.1001 | 100 |
| | mean | 4.36935 | 6.06635 | 12.8022 | 22.665 | 48.5277 | 83.8953 | 100 |
| T | #1 | 9.88627 | 9.71198 | 19.2511 | 63.1759 | 67.3006 | 83.2684 | 100 |
| | #2 | 14.6218 | 13.8625 | 15.0972 | 17.3644 | 26.918 | 67.3275 | 100 |
| | #3 | 5.60944 | 4.43002 | 9.43223 | 15.2589 | 26.967 | 68.4681 | 100 |
| | #4 | 4.59615 | 5.41574 | 10.8573 | 16.9079 | 22.3043 | 71.1139 | 100 |
| | #5 | 7.10343 | 11.7258 | 41.1108 | 98.0032 | 98.7695 | 108.301 | 100 |
| | #6 | 2.93716 | 6.76597 | 32.1214 | 64.4611 | 84.4596 | 87.425 | 100 |
| | mean | 7.45904 | 8.652 | 21.3117 | 45.8619 | 54.4532 | 80.9839 | 100 |

D

| Nycodenz gradient medium (Nycodenz solution:cell suspension) | Nycodenz solution (ml) | cell suspension in GBSS/B (ml) |
|---|---|---|
| 6% - (1:4) | 1.6 | 6.4 |
| 8% - (1:2.57) | 2.24 | 5.76 |
| 10% - (1:1.86) | 2.8 | 5.2 |
| 12% - (1:1.44) | 3.28 | 4.72 |
| 13% - (1:1.22) | 3.6 | 4.4 |
| 14% - (1:1) | 4 | 4 |
| 17% - (1.5:1) | 4.8 | 3.2 |
| 20% - (2.3:1) | 5.6 | 2.4 |

*Nycodenz solution (0.286g/ml): Nycodenz powder in GBSS/A

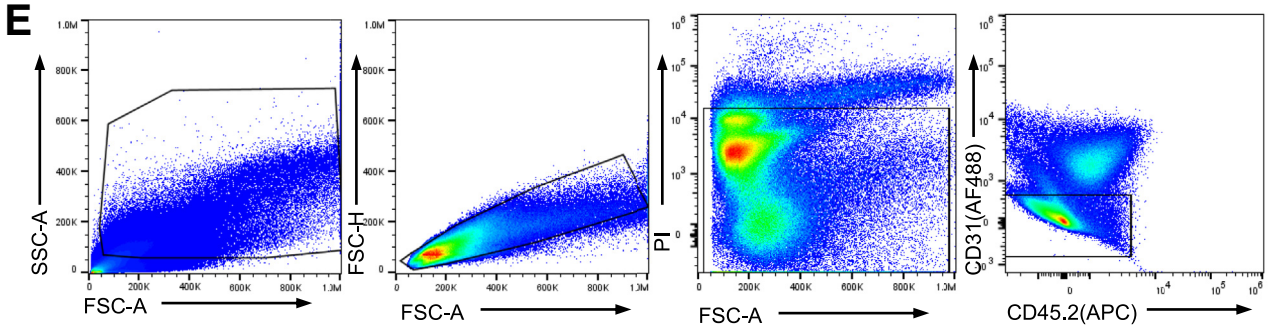


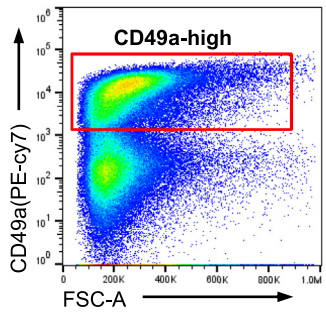


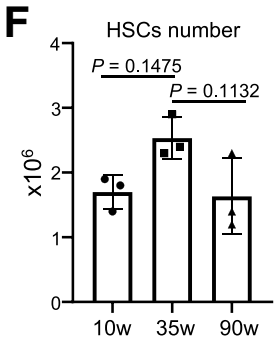


Isolated HSCs number

| HSCs number (x10$^6$) according to age | | | |
|---|---|---|---|
| cells number | 10w | 35w | 90w |
| #1 | 1.8 | 2.9 | 2.3 |
| #2 | 1.4 | 2.3 | 1.4 |
| #3 | 1.9 | 2.4 | 1.2 |
| mean | 1.7 | 2.5 | 1.6 |

**Supplementary Figure 1.** (***See previous page***). **Method for isolating HSCs from the livers of obese mice and mice with obesity-induced HCC.** (*A*–*C*), During the Nycodenz gradient separation, 6% to 17% Nycodenz gradient medium (0.06–0.17 g/mL) was used for further experiments and purification of HSCs. The purified cells in the white layer from NT and T segments were subjected to qPCR analysis for *Lrat* (*A*), *Clec4f* (*B*), or *Stab2* (*C*) expression. Gene expression was normalised to *GAPDH* expression, and data are presented as fold-change difference (n = 6, 13 mice were used in 6 experiments). The average of mouse body weight was 57.6 g (range, 44–67g). The raw data are also shown in the table. (*D*), Nycodenz gradient medium composition. *E*, Flow cytometry gating strategy. *F*, Isolated cell number from 10-, 35-, and 90-week-old mice. The body weight of mice: 10 weeks, 25.9 g; 35 weeks, 31.5 g; 90 weeks, 30.2g. The isolated cell number is shown in the table. Statistical significance was determined using Bonferroni's multiple comparisons test (see the raw data table by the bar graph).

**A**

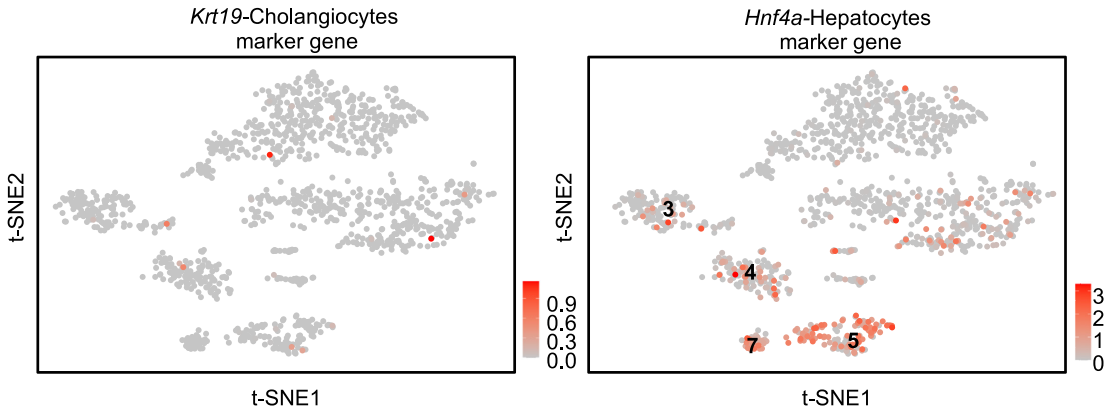


**B**

**HSCs clusters of Normal Diet (ND); HSCs clusters of Non-Tumor (NT); HSCs clusters of Tumor (T)**

| Genes | NT/ND logFC | Genes | T/ND logFC | Genes | T/NT logFC |
|---|---|---|---|---|---|
| ***Itga1*** | -0.8334537 | ***Itga1*** | -1.1696511 | *Ednrb* | -0.2408387 |
| *Plvap* | -0.9490317 | *Plvap* | -1.3609185 | *Tmem204* | -0.3103494 |
| *Ramp1* | -1.0847302 | *Ramp1* | -1.5201724 | ***Itga1*** | -0.3361974 |
| *Ifitm1* | -1.1305634 | *Ifitm1* | -1.5693516 | *Vipr1* | -0.3617078 |
| *Tmem56* | -1.2096658 | *Tmem56* | -1.6243337 | *Plvap* | -0.4118868 |
| *Vipr1* | -1.3899304 | *Vipr1* | -1.7516382 | *Agtr1a* | -0.4123283 |
| *Agtr1a* | -1.3437498 | *Agtr1a* | -1.7560782 | *Tmem56* | -0.4146679 |
| *Ednrb* | -1.5461129 | *Ednrb* | -1.7869516 | *Ramp1* | -0.4354422 |
| *Tmem204* | -1.5865654 | *Tmem204* | -1.8969149 | *Ifitm1* | -0.4387881 |
| *Abcc9* | -1.5228009 | *Abcc9* | -2.0465342 | *Slc43a3* | -0.4660556 |
| *Slc43a3* | -1.7231463 | *Slc43a3* | -2.1892019 | *Abcc9* | -0.5237333 |

**C**

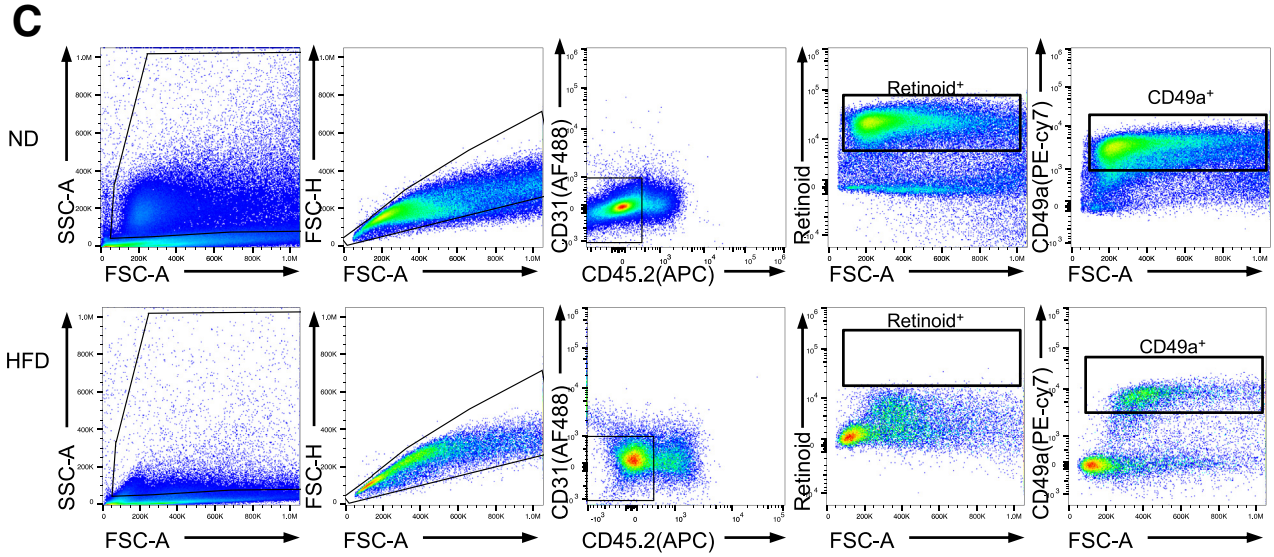


**Supplementary Figure 2. CD49a can be a marker for HSC isolation.** (*A*) Unsupervised t-SNE clustering of the sorted CD31$^-$/CD45.2$^-$ cells revealed the expression of a cholangiocyte marker (*Krt19*) and hepatocyte marker (*Hnf4a*). (*B*) The gene expression in the HSC clusters (ND cluster 0 and 6; NT cluster 1; T cluster 2) was compared and analyzed using log2-Fold change (logFC). The top 11 genes encoding cell surface markers are illustrated in an ascending order of fluctuation. (*C*) Flow cytometry plots of HSCs from ND and HFD mice. The average body weight of mice: ND, 32.6 g (range, 31–34 g; n = 3); HFD, 58.5 g (range, 55–61 g; n = 3).

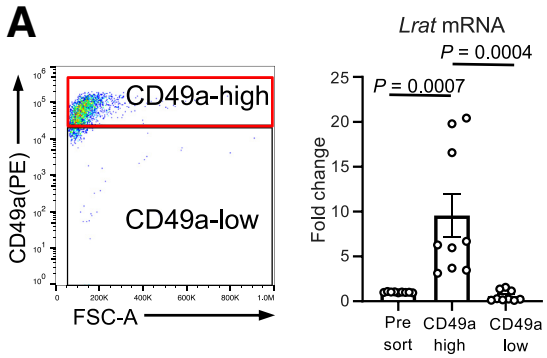


Lrat/GAPDH_db mice

| | pre-sort | CD49a+ | CD49a- |
|---|---|---|---|
| #1-1 | 0.980611 | 6.671992 | 0.275196 |
| #1-2 | 1.082086 | 5.966985 | 0.229644 |
| #1-3 | 0.937303 | 6.281284 | 0.24796 |
| #2-1 | 1.021964 | 3.693979 | 0.159119 |
| #2-2 | 1.040882 | 3.460749 | 0.103542 |
| #2-3 | 0.937154 | 3.115725 | 0.116934 |
| #3-1 | 0.974209 | 20.41387 | 1.146477 |
| #3-2 | 1.020879 | 19.78832 | 1.550025 |
| #3-3 | 1.004912 | 16.56505 | 1.359563 |
| mean | 1 | 9.550884 | 0.576496 |

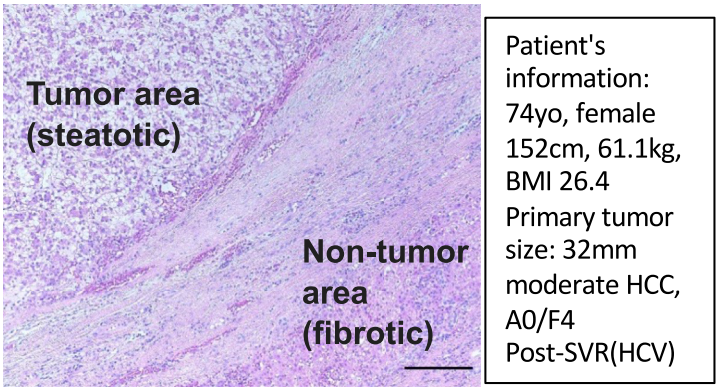


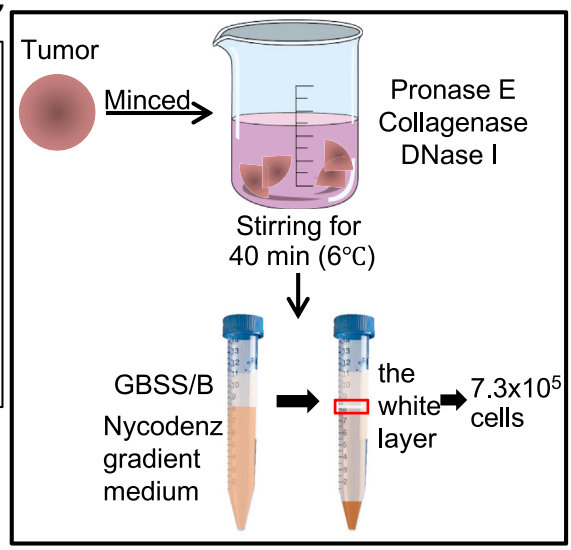


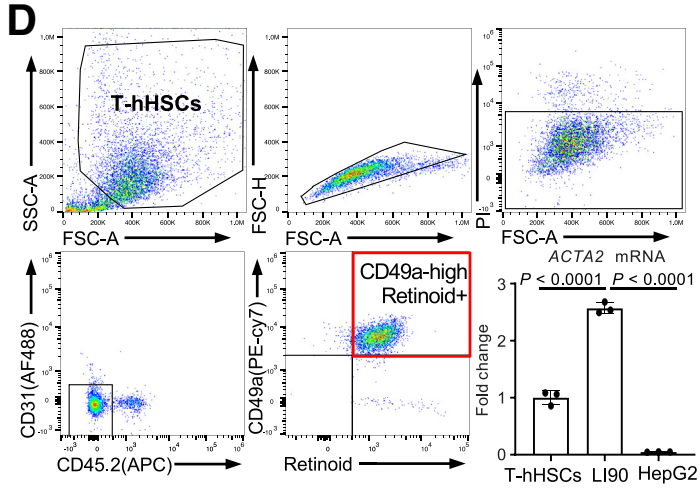


ACTA2/GAPDH_HCC patient

| | T-hHSCs | LI90 | HepG2 |
|---|---|---|---|
| #1 | 0.8562343 | 2.4925383 | 0.0429219 |
| #2 | 1.0833448 | 2.5340178 | 0.0495115 |
| #3 | 1.0604209 | 2.6761511 | 0.0473785 |
| mean | 1 | 2.56757 | 0.0466 |

**Supplementary Figure 3. CD49a-high HSCs can be isolated from the *db/db* mouse liver and the human HCC tissue.** (*A*) Application of the cold isolation protocol for obtaining HSCs from *db/db* mice (n = 3). The average body weight (BW) of mice was 51.8 g (range, 48–57 g). The sorted CD49a-high and CD49a-low cells among $CD31^-/CD45^-$ cells were subjected to qPCR analysis for *Lrat* expression. Data were obtained in triplicate using the samples of 3 different mice and are presented as fold-change difference in comparison with pre-sorted HSCs. Statistical significance was determined using Bonferroni's multiple comparisons test (see the raw data table by the bar graph). (*B*) The histology of post-sustained virologic responce (hepatitis C virus) human HCC tissue (hematoxylin and eosin staining, scale bar, 200 $\mu$m) and the patient's information. (*C*) Method for isolating HSCs from T-hHSCs. (*D*) Flow cytometry analysis and qPCR analysis of T-hHSCs. The rectangle shows the double-positive fraction of CD49a expression and retinoid content. T-hHSCs, LI90 (human HSC line), or HepG2 (human HCC cell line) cells were subjected to qPCR analysis for evaluating *ACTA2* expression. Data were obtained in triplicate using these samples. Statistical significance was determined using Bonferroni's multiple comparisons test (see the raw data table by the bar graph).

**Supplementary Table 1A.** Solutions

| Solutions | Reagents | Final concentration |
|---|---|---|
| EGTA perfusion solution | NaCl | 136.89 mM |
| | KCl | 5.37 mM |
| | $NaH_2PO_4$ | 0.64 mM |
| | $Na_2HPO_4$ | 0.85 mM |
| | HEPES | 9.99 mM |
| | NaHCO3 | 4.17 mM |
| | EGTA | 0.50 mM |
| | Glucose | 5.00 mM |
| Enzyme buffer | NaCl | 136.89 mM |
| | KCl | 5.37 mM |
| | $NaH_2PO_4$ | 0.64 mM |
| | $Na_2HPO_4$ | 0.85 mM |
| | HEPES | 9.99 mM |
| | NaHCO3 | 4.17 mM |
| | $CaCl_2 \cdot 2H_2O$ | 3.81 mM |
| Gey's balanced salt solution B, GBSS/B | NaCl | 136.89 mM |
| | KCl | 4.96 mM |
| | $MgCl_2 \cdot 6H_2O$ | 1.03 mM |
| | $MgSO_4 \cdot 7H_2O$ | 0.28 mM |
| | $Na_2HPO_4$ | 0.42 mM |
| | $KH_2PO_4$ | 0.22 mM |
| | Glucose | 5.50 mM |
| | NaHCO3 | 2.70 mM |
| | $CaCl_2 \cdot 2H_2O$ | 1.53 mM |
| Gey's balanced salt solution A, GBSS/A | KCl | 4.96 mM |
| | $MgCl_2 \cdot 6H_2O$ | 1.03 mM |
| | $MgSO_4 \cdot 7H_2O$ | 0.28 mM |
| | $Na_2HPO_4$ | 0.42 mM |
| | $KH_2PO_4$ | 0.22 mM |
| | Glucose | 5.50 mM |
| | NaHCO3 | 2.70 mM |
| | $CaCl_2 \cdot 2H_2O$ | 1.53 mM |
| Pronase E perfusion solution | Pronase E in enzyme buffer | 1 mg/mL |
| Collagenase perfusion solution | Collagenase in Enzyme buffer | 1.33 mg/mL |
| In vitro digestion solution | Pronase E | 0.556 mg/mL |
| | Collagenase | 0.556 mg/mL |
| | DNase I in Enzyme buffer | 0.02 mg/mL |

**Supplementary Table 1B.** Chemicals

| Reagents | Company, catalog number |
|---|---|
| Pronase E | Sigma-Aldrich, cat. no. 1.07433 |
| Collagenase | Wako, cat. no. 032-22364 |
| DNaseI | Roche, cat. no. 11284932001 |
| Nycodenz AG | AXS, cat. no. 1002424 |
| EGTA | NACALAI, cat. no. 15214-92 |
| Sodium chloride (NaCl) | Wako, cat. no. 191-01665 |
| Potassim chloride (KCl) | NACALAI, cat. no. 28514-75 |
| Sodium | NACALAI, cat. no. 31720-65 |
| di-Sodium | NACALAI, cat. no. 31726-05 |
| HEPES | DOJINDO, cat. no. 340-01371 |
| Sodium bicarbonate | NACALAI, cat. no. 31212-25 |
| d-(+)-Glucose | NACALAI, cat. no. 16806-25 |
| Calcium chloride | NACALAI, cat. no. 06731-05 |
| Magnesium chloride | NACALAI, cat. no. 20909-55 |
| Magnesium sulfate | NACALAI, cat. no. 21003-75 |
| Potassium phosphate | NACALAI, cat. no. 28721-55 |
| RBC lysis buffer (10×) | Biolegend, cat. no. 420302 |
| D-PBS (−) | FUJIFILM, cat. no. 045-29795 |

**Supplementary Table 1C.** Equipment

| Equipment | Company, catalog number |
|---|---|
| Perfusion pump | Cole-Parmer, 07516-10 |
| Perfusion line | Cole-Parmer, 06424-14 |
| 24-gauge catheter | TERUMO SURFLO, SR-OT2419CP |
| 70-$\mu$m Cell strainer | AS ONE, 3-6649-02 |
| Water bath | THERMAL ROBO, TR-1AR |
| Bottle-top filter, 0.45 $\mu$m | Thermo scientific, cat. no. 291-3345 |
| Refrigerated benchtop | Beckman Coulter, Allegra X-15R |
| Cell sorter | SONY-SH800, cat. no. SH800S |
| Attune NxT Acoustic | Thermo Fisher, cat no. A24860 |

**Supplementary Table 1D.** Primers

| Gene | Primer sequences |
|---|---|
| Mouse GAPDH | 5'-CAACTACATGGTCTACATGTTC-3' (forward)<br>5'-CACCAGTAGACTCCACGAC-3' (reverse) |
| Mouse *Lrat* | 5'-TACTGCAGATATGGCTCTCG-3' (forward)<br>5'-GATGCTAATCCCAAGACAGC-3' (reverse) |
| Mouse Clec4f | 5'-TGCAGGAAGCTGTGGCTGCA-3' (forward)<br>5'-TCCCGCCACGGCTTCTTGTC-3' (reverse) |
| Mouse Stab2 | 5'-ATTGCCTCTAACGGGGTTCT-3' (forward)<br>5'-ATCGCACCAGTAACCAGGAC-3' (reverse) |
| Mouse albumin | 5'-CCCGAAGCTTGATGGTGTGA-3' (forward)<br>5'-GTCTGGCTCAGACGAGCTAC-3' (reverse) |
| Human Acta2 | 5'-ACCTCATGAAGATCCTGACT-3' (forward)<br>5'-TTCAAAGTCCAGAGCTACAT-3' (reverse) |
| Human GAPDH | 5'-GTGGTCTCCTCTGACTTCAAC-3' (forward)<br>5'-TGAGCTTGACAAAGTGGTCG-3' (reverse) |

**Supplementary Table 1E.** Antibodies

| Antibodies | Company, catalog number |
|---|---|
| CD16/32 mAb (2.4G2) | BioXcell, #BE0307 |
| CD31 | Biolegend, #102514 |
| CD45.2 | Biolegend, #109813 |
| CD49a | Biolegend, #142603 |
| Propidium iodide | Biolegend, #421301 |